

Frequency Response Analysis of Deep Groove Ball Bearing

K. Raghavendra¹, Karabasanagouda .B .N²

¹Assistant Professor, Department of Mechanical Engineering,
Bellary Institute of Technology & Management, Bellary, VTU Belgaum, Karnataka, India

²M. Tech Student, Department of Mechanical Engineering,
Bellary Institute of Technology & Management, Bellary, VTU Belgaum, Karnataka, India

Abstract: *The study investigated the variation of statistical parameters of vibration signals acquired from ball bearings with respect to speed using an experimental set up. Accelerometers mounted on the bearing housing and connected to Multi function FFT Vibration Analyzer (CSI) 2130 were used to measure the radial, axial & vertical accelerations from the bearing housing. The RMS value & Kurtosis analysis validates that the ball bearing health can be fairly monitored using frequency domain analysis. The method proves to be a simple, quick & cost effective method in the condition monitoring of ball bearings & is most suitable for random signals such as from bearings.*

Keywords: FFT Vibration Analyzer (CSI) 2130, RMS Value, Kurtosis analysis, Ball bearing health, Random signals

1. Introduction

Maintenance cost is one of the major operating costs in manufacturing companies. It involves spare parts cost, breakdown cost and manpower cost. Unexpected breakdowns, replacement and repair expenses from catastrophic failures indulge in loss of output due to machinery downtime.

Adoption of predictive and preventive maintenance procedures significantly reduces these losses. This is essential in maintenance management to enhance the product quality. Predictive maintenance requires continuous measurement of machine operating parameters such as temperature, power consumption, vibration, noise, forces. A Condition Based Monitoring (CBM) program consists of three key steps as shown in Figure 1.

- Data acquisition** (Information collecting): A data or signal relevant to system health is collected.
- Data processing** (Information handling): A data or signal collected is analyzed for its better interpretation.
- Maintenance** (Decision making): Here, efficient maintenance policies are recommended.

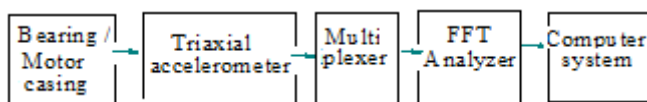


Figure 1: Steps in CBM

N. Tandon et al. [i] in 1997 proposed an analytical model for predicting the vibration frequencies of rolling bearings and the amplitudes of significant frequency components due to a localized defect on outer race or inner race or on one of the rolling elements under radial and axial loads. Arnaz S. Malhi [ii] in 2002 did a preliminary vibration analysis of a rolling element passing over a single point defect on the outer ring of a ball bearing using FEA software ANSYS. Author extracted vibration signals for two different defect sizes and proposed an index for comparison of different defect sizes.

Sadettin Orhan et al. [iii] in 2005 presented vibration monitoring and analysis case studies and examined those in machineries that were running in real operating conditions using spectral analysis.

Robert B. Randall et al.[iv] in 2010 presented a tutorial to guide the reader in the diagnostic analysis of acceleration signals from rolling element bearings in the presence of strong masking signals from other machine components such as gears. M.S.Patil et al. [v] in 2010 presented an analytical model for predicting the effect of a localized defect on the ball bearing vibrations. Authors also investigated the effect of the defect size and its location on the ball bearing vibrations. Sylvester A. Aye [vi] in 2011 investigated on the sensitivity of using a contact and a non contact method in condition monitoring of taper roller bearings.

2. Material and Methodology

An experimental set up developed is as shown in Figure 2. A shaft is supported by two test bearings at its end which is driven by an AC motor and varying speed by electrical drive. A three jaw coupling connects motor to the system to achieve higher speeds of rotation. CSI-2130 vibration analyzer is used to pick up the acceleration signals. The signals for healthy and faulty bearings were obtained for various speeds with different unbalance mass on the shaft.



Figure 2.1: Experimental Setup for Deep Groove Ball Bearing Test

The block diagram of instrumentation is as shown in Figure 4.2. It consists of an acceleration sensor, FFT spectrum analyzer, electrical drive and a digital tachometer. Acceleration sensor has a magnetic base for mounting on the bearing housing and the other end is connected to the FFT spectrum analyzer. FFT spectrum analyzer is used to record the corresponding vibration spectrum. Electrical drive is used for varying the voltage supplied to AC motor to vary its speed. A digital tachometer is used to measure different shaft speeds.

2.1 Instrumentation

Vibration signal from bearing was acquired with a tri-axial accelerometer of sensitivity 5mV/g mounted on bearing housing. The time domain waveform is acquired in radial and axial direction at different speeds. These vibration signals were analyzed in lab view software. Fig. 4.3 shows the lab view program for spectral analysis of vibration signal and evaluating Kurtosis values.

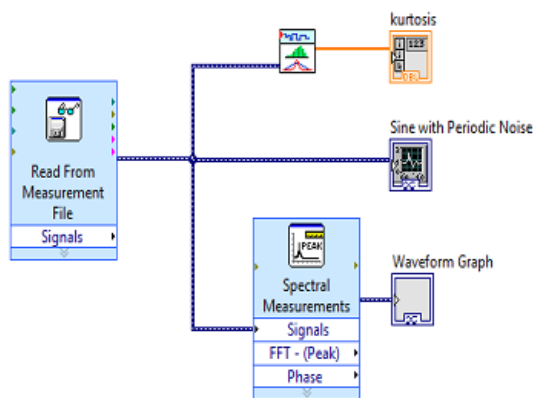


Figure 2.2: Lab view program for spectral analysis and kurtosis

2.2 Measurement Conditions

Vibration data from the bearing was acquired at different speeds such as 300, 900, 1500, 2100 and 2500 rpm. The load on the bearing was considered constant on defect free bearing. It is observed that with variation of load on bearing, the amplitude of the vibration changes.

The defect to the outer race of nondrive side test bearing was produced by pencil grinding. It consists of an uneven surface of 0.4 mm depth and 2 mm width diameter to the inner race of a bearing as shown in Figure 4.3



Figure 2.3: Deep groove ball bearing inner race surface wear induced

3. Bearing Characteristics Frequencies

A machine with a rolling element bearing is running at certain speed; when a defect begins to develop, the vibration spectrum changes produced in bearing. The occurrence frequencies of the shocks resulted from the defects in the bearings are called bearing defect frequencies or bearing characteristics frequencies. Each bearing element has a bearing characteristic frequency. The peaks will occur in the spectrum at these frequencies due to increase in vibrational energy. Initiation and progression of defects or faults on rolling element bearing generate specific and predictable characteristic of vibration. A model presented by Tandon and Choudhury [i], predicted frequency spectrum having peaks at these frequencies. Defects in components of rolling element bearing such as inner race, outer race, rolling elements and cage generate a specific defect frequencies calculated theoretically from the below equations:

(a) FTF - Fundamental Train Frequency (frequency of the defected cage):

$$f \text{ (Hz)} = \frac{1}{2} \times \omega_1 \times \left(1 - \frac{B_d}{P_d} \times \cos \theta \right) \dots\dots\dots(1)$$

(b) BPFI - Ball Pass Frequency of the Inner race (frequency produce when the rolling elements roll across the defect of inner race):

$$f \text{ (Hz)} = \frac{n}{2} \times \omega_1 \times \left(1 + \frac{B_d}{P_d} \times \cos \theta \right) \dots\dots\dots(2)$$

(c) BPFO – Ball Pass Frequency of Outer race (frequency produce when the rolling elements roll across the defect of outer race):

$$f \text{ (Hz)} = \frac{n}{2} \times \omega_1 \times \left(1 - \frac{B_d}{P_d} \times \cos \theta \right) \dots\dots\dots(3)$$

(d) BSF – Ball Spin Frequency (circular frequency of each rolling element as it spins):

$$f \text{ (Hz)} = \omega_{rp} = \frac{P_d}{2B_d} \times \omega_1 \times \left(1 - \frac{B_d}{P_d} \times (\cos \theta)^2 \right) \dots\dots\dots(4)$$

(e) Rolling Element Defect Frequency or 2 x BSF

$$f \text{ (Hz)} = \frac{P_d}{B_d} \times \omega_1 \times \left(1 - \frac{B_d}{P_d} \times (\cos \theta)^2 \right) \dots\dots\dots(5)$$

Theoretical calculation of the above listed frequencies at different Speeds (RPM) is shown in Table I.

$$\omega_{rp} = \frac{\omega_1 \times P_d \times \left[1 - \left(\frac{B_d}{P_d} \times \cos \theta \right)^2 \right]}{2B_d} \dots\dots\dots(6)$$

Table 3.1: Details of Deep Groove Ball Bearing

1	Rotational frequency	ω_i
2	Ball or roller diameter	$B_d = 8.7 \text{ mm}$
3	Number of balls of rollers	$n = 8 \text{ No's}$
4	Pitch Diameter	$P_d = 38.3 \text{ mm}$
5	Contact Angle	$\theta = 0 \text{ degree}$
6	Inner Diameter	$d = 24.8 \text{ mm}$
7	Outer Diameter	$D = 51.8 \text{ mm}$
8	Width of the Bearing	$W = 12.5 \text{ mm}$
9	Bearing Model	FAG 6204

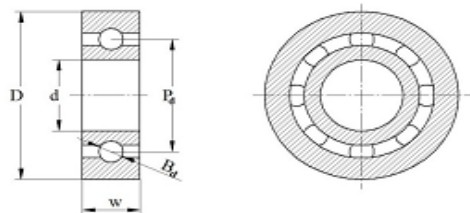


Figure 4.6: Deep groove ball bearing nomenclatures

Table 3.2: Theoretical calculation of the frequencies at different speeds

RPM	Rotational Frequency (Hz)		Defect Frequency (Hz)			
	ω_i	ω_e	ω_c	ω_{ip}	ω_{cp}	ω_{rp}
300	5.2	0	16.218	11.232	25.38	22.464
600	10.1	0	31.502	21.816	49.298	43.632
900	15.1	0	47.097	32.616	73.703	65.232
1500	25.1	0	78.287	54.516	122.513	108.433
2100	35.2	0	109.476	75.817	171.324	151.633
2500	41.8	0	130.374	90.289	204.026	180.577

Firstly, vibration signals collected in the form of time domain are converted into frequency domain by processing Fast Fourier Transform (FFT) on each of the bearings. The RMS values and Kurtosis values computed from the frequency domain signals and amplitude of vibration at predominant frequencies are considered for the analysis. The results of various frequency responses are presented and discussed in this paper.

4. Results and Discussion

4.1 Observed Spectra

For each case, the spectrum was recorded for 6 different shaft Speeds. The observed acceleration spectra for each of the six cases are as shown in the following Figures.

4.1.1 Case I: Healthy Bearing with No Bolt (Speed=2664rpm)

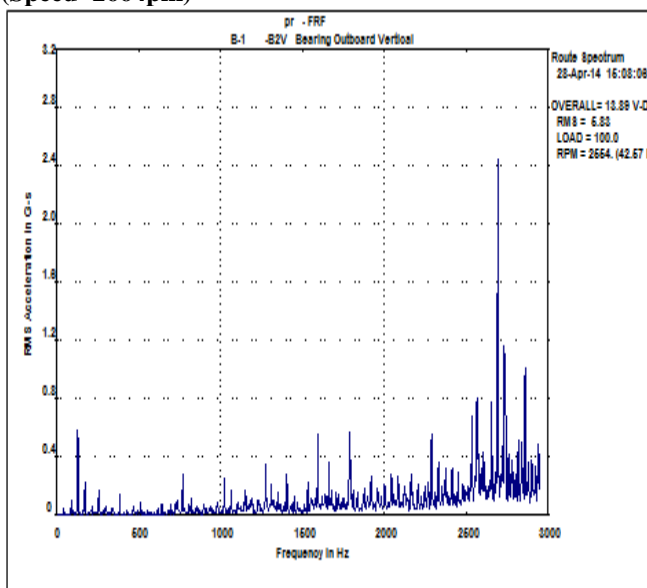


Figure 4.1: Acceleration Spectrum for Case I at 2664 rpm

4.1.2 Case II: Healthy Bearing with One Bolt (Speed=2462rpm)

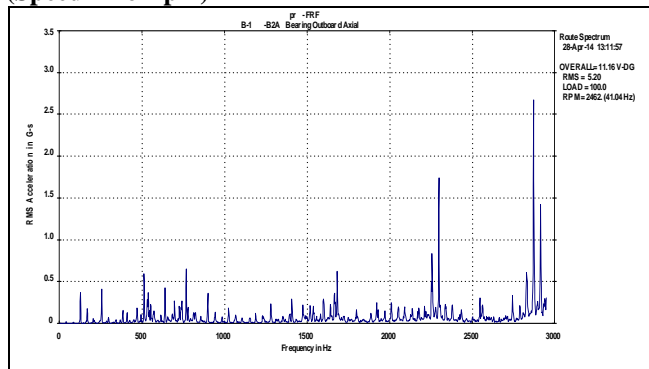


Figure 4.2: Acceleration Spectrum for Case II at 2462 rpm

4.1.3 Case III: Healthy Bearing with Two Bolt (Speed=2448rpm)

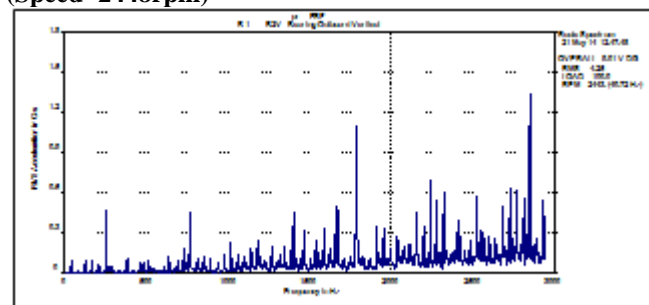


Figure 4.3: Acceleration Spectrum for Case III at 2448 rpm

4.1.4 Case IV: Defective Bearing with No Bolt (Speed=2048rpm)

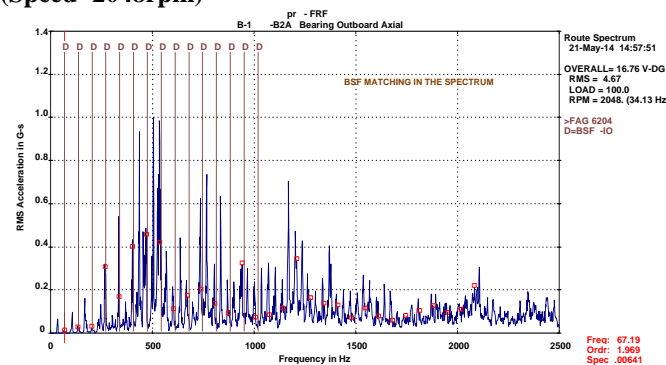


Figure 4.4: Acceleration Spectrum for Case IV at 2048 rpm

4.1.5 Case V: Defective Bearing with One Bolt (Speed=2601rpm)

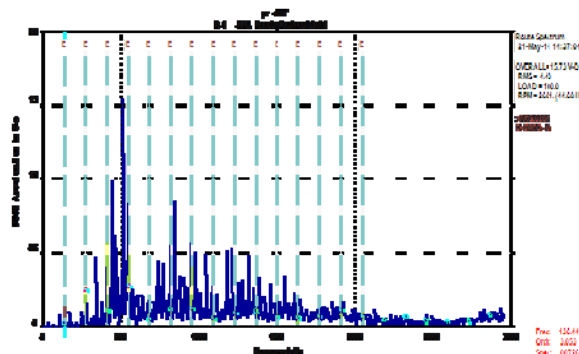


Figure 4.5: Acceleration Spectrum for Case V at 2601 rpm

4.1.6 Case VI: Defective Bearing with Two Bolt (Speed=2681rpm)

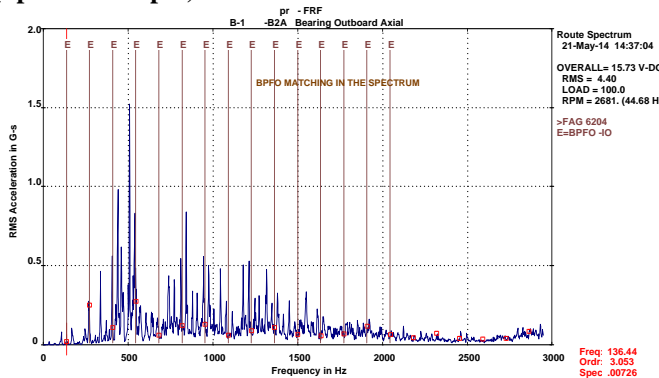


Figure 4.6: Acceleration Spectrum for Case VI at 2681 rpm

Table 4.1: Theoretical calculation of the defective frequencies at maximum speeds

RPM	Rotational Frequency (Hz)	Fundamental frequency obtained from statically			Fundamental frequency obtained from FFT analyzer		
		BPFI	BPFO	BSF	BPFI	BPFO	BSF
2048	34.13	167.53	105.51	71.25	168.89	102.91	67.99
2601	44.01	216.03	136.05	91.86	217.78	132.69	87.67
2681	44.68	219.32	138.12	93.27	221.09	134.71	89.00

Inference from the Experimental Results

- 1) Fig. 4.4, 4.5 and 4.6 shows the frequency domain waveform for the defective bearing with defect on inner race at maximum speed of 2048rpm, 2601rpm, 2681 rpm and FFT spectrum respectively in axial and radial directions. It is observed that the spectrum clearly shows the presence of fault on the inner race and the balls. The theoretical frequency 167Hz, 216Hz and 219Hz, obtained by equations mentioned in section 4.5 closely matches with the fault frequencies obtained from FFT analyzer. Hence the frequency domain approach gives precise estimation of location of defects.
- 2) The theoretical frequency for the inner race defect closely matches with the experimental one.
- 3) Fig. 4.1,4.2 and 4.3 shows the frequency domain waveform for the healthy bearing at maximum speed of 2462rpm,2541rpm and 2443rpm and FFT spectrum respectively in axial and radial directions. It is observed that the spectrum clearly shows for no bolt condition have peak RMS acceleration at frequency of 2750Hz, for one bolt condition have peak RMS acceleration at frequency of 2350Hz and 2850Hz and for two bolt condition have peak RMS acceleration at frequency of 1800Hz it reveals that the maximum speed of the bearing at which the shaft can produce minimal noise.

RMS Value

For a dispersed data having N number of data points and X_m as an arithmetic mean, a root mean square value is defined as square root of sum of squares of all deviation values divided the by number of samples, where X_i is i^{th} data point.

$$RMS = \sqrt{\sum_{i=1}^N \frac{(X_i - X_m)^2}{N}} \dots \dots \dots (7)$$

Kurtosis Value

For a dispersed data having N number of data points and X_m as arithmetic mean, a Kurtosis is a measure of peakedness of the probability distribution of a real valued random variable. Kurtosis is a measure of whether the data are peaked or flat relative to a normal distribution. The kurtosis is calculated by following formula;

$$Kurtosis = \frac{\sum_{i=1}^N \frac{(X_i - X_m)^4}{N}}{RMS^4} \dots \dots \dots (8)$$

Where $X_i = i^{th}$ Data Point, RMS = Root Mean Square Value

4.2 RMS Value and Kurtosis Analysis

The data points and variation of RMS and Kurtosis values of acceleration with speed for the Case I is given in Table 4.2 and Figure 4.7 respectively.

4.2.1 Case I : Healthy bearing with no bolt

Table 4.2: Data points for RMS and Kurtosis values of acceleration with speed

Speed(RPM)	RMS value(m/s ²)	Kurtosis value
300	0.1	0.156
600	1.3	-0.223
900	1.4	-0.034
1500	2.0	-0.327
2100	3.9	-0.323
2500	5.2	-0.102

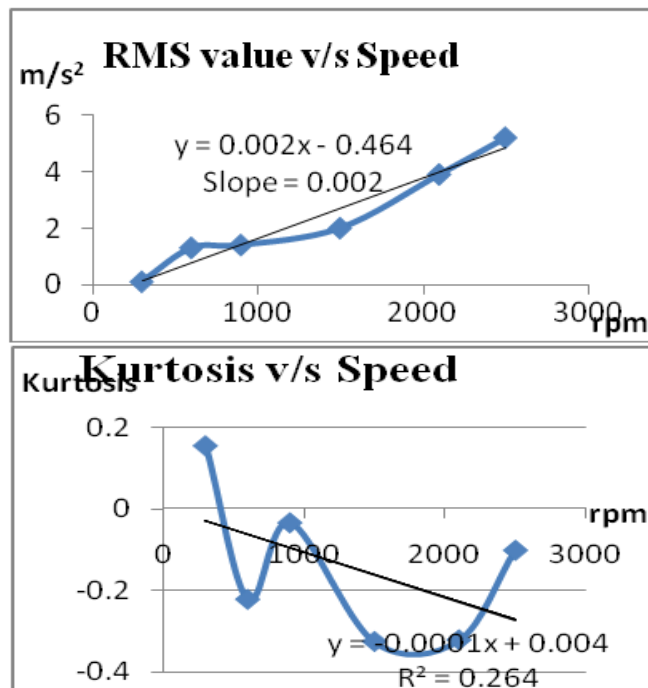


Figure 4.7: Variation of RMS and Kurtosis values with speed and their “Best Fit” for Case I

The data points and variation of RMS and Kurtosis values of acceleration with speed for the Case II are given in Table 4.3 and Figure 5.8 respectively.

4.2.2 Case II: Healthy bearing with one bolt

Table 4.4: Data points for RMS and Kurtosis values of acceleration with speed

Speed(RPM)	RMS value(m/s ²)	Kurtosis value
300	0.06	-0.055
600	0.92	-0.182
900	1.0	-0.165
1500	2.2	0.423
2100	2.4	-0.133
2500	3.6	0.685

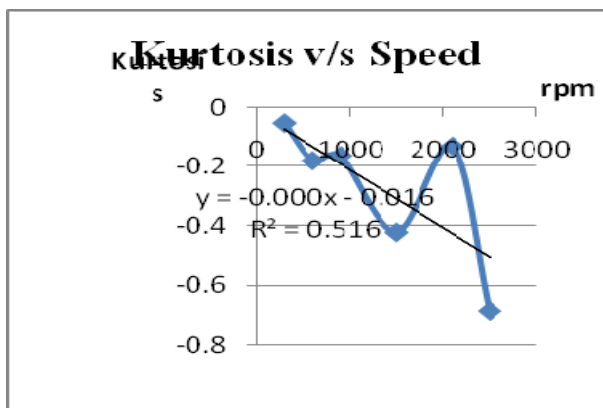


Figure 4.8: Variation of RMS and Kurtosis values with speed and their “Best Fit” for Case II

The data points and variation of RMS and Kurtosis values of acceleration with speed for the Case II are given in Table 4.4 and Figure 4.8 respectively.

4.2.3 Case III: Healthy bearing with two bolts

Table 4.5: Data points for RMS and Kurtosis values of acceleration with speed

Speed(RPM)	RMS value(m/s ²)	Kurtosis value
300	0.13	-0.651
600	0.72	-0.237
900	1.7	-0.265
1500	2.2	-0.073
2100	2.4	-0.204
2500	3.4	-0.366

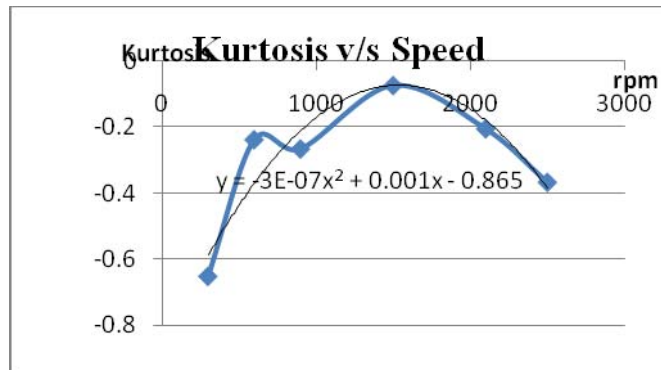
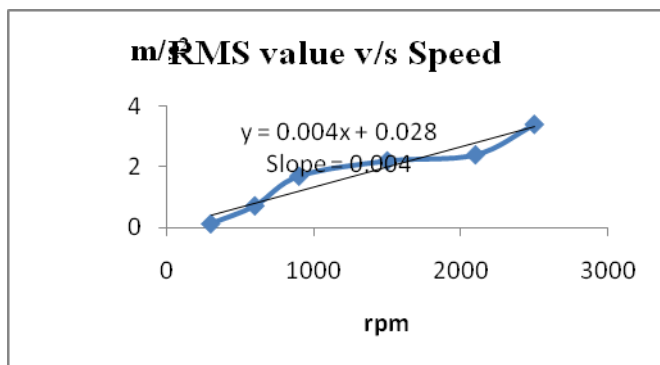


Figure 4.9: Variation of RMS and Kurtosis values with speed and their “Best Fit” for Case II

The data points and variation of RMS and Kurtosis values of acceleration with speed for the Case II are given in Table 4.5 and Figure 4.9 respectively.

4.2.4 Case IV: Defective bearing with no bolt

Table 4.5: Data points for RMS and Kurtosis values of acceleration with speed

Speed(RPM)	RMS value (m/s ²)	Kurtosis value
300	0.14	1.456
600	0.4	1.895
900	1.4	0.654
1500	3.1	0.183
2100	4.4	0.288
2500	8.4	0.464

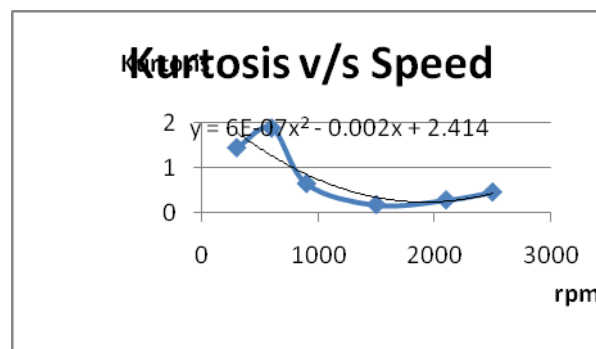
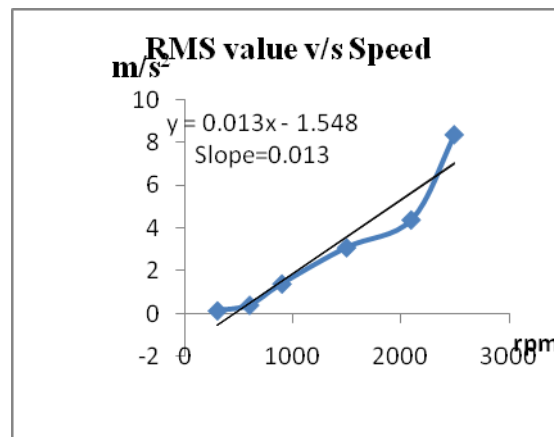


Figure 4.10: Variation of RMS and Kurtosis values with speed and their “Best Fit” for Case IV

The data points and variation of RMS and Kurtosis values of acceleration with speed for the Case II are given in Table 4.6 and Figure 4.11 respectively.

4.2.5 Case V: Defective bearing with one bolt

Table 4.6: Data points for RMS and Kurtosis values of acceleration with speed

Speed(RPM)	RMS value(m/s ²)	Kurtosis value
300	0.1	1.595
600	0.8	2.057
900	1.8	-0.070
1500	4.0	0.300
2100	4.6	0.380
2500	7.8	0.305

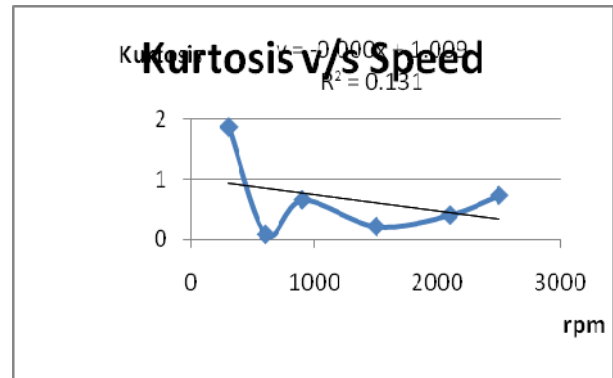
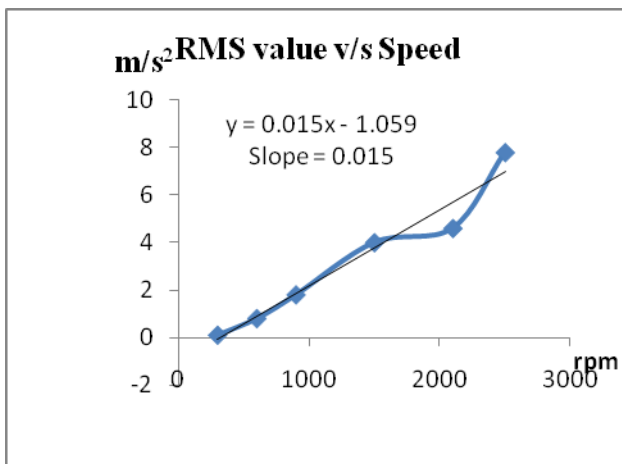
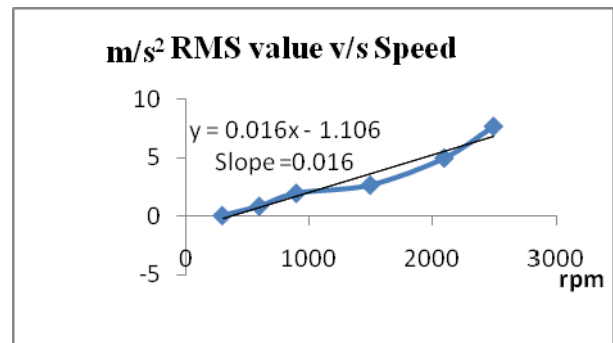


Figure 4.12: Variation of RMS and Kurtosis values with speed and their “Best Fit” for Case VI

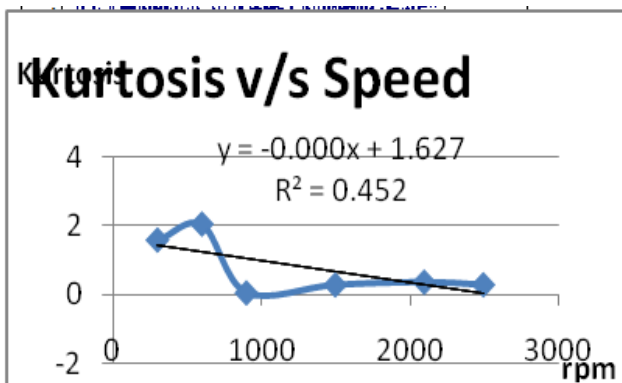


Figure 4.11: Variation of RMS and Kurtosis values with speed and their “Best Fit” for case V

The data points and variation of RMS and Kurtosis values of acceleration with speed for the case II are given in Table 5.7 and Figure 5.12 respectively.

4.2.6 Case VI: Defective bearing with two bolt

Table 4.7: Data points for RMS and Kurtosis values of acceleration with speed

Speed(RPM)	RMS value(m/s ²)	Kurtosis value
300	0.1	1.867
600	0.9	0.076
900	2.0	0.653
1500	2.7	0.207
2100	5.0	0.397
2500	7.7	0.728

Inference

a) From the above figures it is seen that the values of Kurtosis for healthy bearing is close to 0 with negative values which indicate the fault free state of the bearing. For defects on the inner race lies with positive values between 0.1 and 3. This is the clear indication of the defects in the bearing.

4.3 Inference from RMS Value and Kurtosis Analysis

Table 4.8 shows the slopes of RMS value v/s speed “Best Fit” curve for the six cases considered.

Table 4.8: Slopes of RMS value v/s speed “Best fit” curves for the six cases

Case	Description	Slope of the RMS value v/s Speed “Best fit”
I	Healthy bearing with No Bolt	0.002
II	Healthy bearing with One Bolt	0.001
III	Healthy bearing with Two Bolt	0.004
IV	Defective bearing with No Bolt	0.013
V	Defective bearing with One Bolt	0.015
VI	Defective bearing with Two Bolt	0.016

Inference

- 1) For healthy bearings, slope of the RMS Value v/s Speed best fit curve gradually increases as unbalance increases.
- 2) As the defect is introduced in the bearing, the corresponding slope values shoot approximately to 10 times of their values for healthy bearings subjected to same unbalance.

Table 4.8: Regression Values of Kurtosis v/s Speed “Best fit” curves for the six case

Case	Description	Regression value of the Kurtosis v/s Speed “Best fit”
I	Healthy bearing with No Bolt	0.264
II	Healthy bearing with One Bolt	0.516
III	Healthy bearing with Two Bolt	--
IV	Defective bearing with No Bolt	--
V	Defective bearing with One Bolt	0.452
VI	Defective bearing with Two Bolt	0.131

Inference

1. For healthy bearings, regression values of the Kurtosis v/s speed best fit curve decreases with unbalance. The trend is reverse of the trend of RMS Values with speed. This can be validated by the Equation (7).

$$Kurtosis = \frac{\sum_{i=1}^N (x_i - \bar{x})^2}{RMS^4} \dots\dots\dots (7)$$

2. For defective bearings, regression value of the Kurtosis v/s speed best fit curve decreases with unbalance.
 3. Bearing signals are not periodic but stochastic (or random) having indeterminacy. This allows them to be separated from deterministic signals such as from gears [v]. Thus, the kurtosis curves reflect an uncertainty in their trend.

5. Conclusion

The development of bearing condition monitoring test rig was successfully carried out which can be used to determine the health of a bearing used in the rotating machinery. The RMS value analysis validates that the ball bearing health can be fairly monitored using frequency domain analysis. The Proposed Statistical analysis proves to be a simple, quick and cost effective method in the condition monitoring of ball bearings. The method proves to be most suitable for random signals obtained from bearings. The RMS value shows that as the speed increases, the magnitude of vibration response also increases. Additionally, the Kurtosis value for new bearing is close to 0 with negative values which is a clear indication that no defects in the bearing. For inner race defect the value lies with positive values between 0.1 and 3, indicating moderate defect in the bearing. Hence kurtosis value shows the state of the bearing.

Based on the studies carried out on frequency response analysis of Deep groove ball bearings, it can be concluded that FFT spectrum indicate the location of the fault. Additionally, Kurtosis, one of the statistical parameters is evaluated for the above cases of the defects on the bearing. Kurtosis though indicates state of the bearing; it cannot detect the location of faults. Also, it is not suitable for detecting fault on outer race of rolling bearing. The results reveal that vibration based monitoring method is effective in detecting the faults in the bearing.

The RMS value analysis validates that the ball bearing health can be fairly monitored using frequency domain analysis. The proposed statistical analysis proves to be a simple, quick

and cost effective method in the condition monitoring of ball bearings.

Experimental study reveals the frequency response analysis is an effective tool in analyzing the frequency signal obtained from bearing in order to characterize and condition monitoring of rotary equipments.

References

- [1] N. Tandon and A. Choudhury, “A review of vibration and acoustic measurement methods for the detection of defects in rolling element bearings”, Tribology International, Vol.32.(1999), 12th October 1999, Pp.469-480.
- [2] N. Tandon and A. Choudhury, ‘A theoretical model to predict vibration response of rolling bearings to distributed defects under radial load’ Journal of Vibrations and Acoustics, Vol. 120, pp. 214-20, 1998.
- [3] N. Tandon and A. Choudhury, ‘An analytical model for the prediction of the vibration response of rolling element bearings due to a localized defect’ Journal of Sound and Vibration, Vol. 205, No. 3, pp. 275-92, 1997.
- [4] Arnaz S. Malhi, Finite element modelling of vibrations caused by a defect in the outer ring of a ball bearing, Proceedings of ASME on Finite Element Method and Applications, Vol.605. Amherst, Elab, Spring 2002, Pp.1-6.
- [5] Sadettin Orhan, Nizami Akturk, Veli Celik, Vibration monitoring for defect diagnosis of rolling element bearings as a predictive maintenance tool: Comprehensive case studies, NDTandE International, Vol.39.(2006), 29th August 2005, Pp.293-298.
- [6] Robert B. Randall and Jerome Antoni, Rolling element bearing diagnostics -A Tutorial, Mechanical Systems and Signal Processing, Vol. 25.(2011), 29th July 2010, Pp. 485-520.
- [7] M.S. Patil, Jose Mathew, P.K. Rajendrakumar and Sandeep Desai, A theoretical model to predict the effect of localized defect on vibrations associated with ball bearing, International Journal of Mechanical Sciences, Vol.52.(2010), 17th May 2010, Pp.1193-1201.
- [8] Sylvester A. Aye, Statistical Approach for Tapered Bearing Fault Detection using Different Methods, Proceedings of the World Congress on Engineering, Vol. III (2011), London, U.K., July 6-8, 2011.
- [9] I.E. Alguindigue, A.L. Buczak and Robert E. Uhrig, ‘Monitoring and Diagnosis of Rolling Element Bearings Using Artificial Neural Networks’ IEEE Transactions on Industrial Electronics, Vol. 40, No. 2, pp. 209-217, April 1993.
- [10] Y.T. Su and S.J. Lin, ‘On initial fault detection of a tapered roller bearing: Frequency domain analysis’ Journal of Sound and Vibration, Vol. 155, No. 1, pp 75-84, 1992.
- [11] Emerson manual for ball bearing condition monitoring.
- [12] H. Prasad, ‘The effect of cage and roller slip on the measured defect frequency response of rolling element bearings’ ASLE Trans., Vol. 30, No3, pp. 360-7, 1987.
- [13] Tandon, N. —A comparison of some Vibration parameters for the condition monitoring of rolling element bearings. Measurement, 12: 1994, pp. 285-289.
- [14] Zeki Kiral, Hira Karaguille. —Simulation and analysis of vibration signals generated by rolling element bearing with defects. Tribology International, 36: pp. 667- 678, 2003.